Dynamics and control implementation of a supercritical CO_2 simple recuperated cycle

Simone Maccarini[1*], *Swatara* Tucker[1], *Luca* Mantelli[1], *Stefano* Barberis[1], *Alberto* Traverso[1]

[1]Thermochemical Power Group (TPG), DIME, Università degli Studi di Genova, Genova, Italy

Abstract. Interest in supercritical CO2 power cycles is constantly increasing, showing good efficiency, and promising competitive costs and enhanced flexibility with respect to competing systems. Some project within the EU Horizon 2020 program have studied these systems and aim to demonstrate them in large scale, following the example of the STEP project in US. This work is part of the effort of the SOLARSCO2OL project to build a sCO2-CSP power demo plant at MW scale.
A dynamic model of a simple recuperated sCO2 cycle is developed in TRANSEO, using miniREFPROP to compute fluid properties, and table of properties are implemented, when possible, to enhance the performance of the code. Control logics is described and simple controllers implemented.
Finally, controllers are tested showing the response of the main parameters of the plant to a ramp variation of the load. Stable compressor inlet pressure is achieved with an inventory control, while a stable turbine inlet temperature allows a high efficiency in part-load operation.

1 Introduction

The use of supercritical CO_2 (sCO2) for power application has become an important trend in research and development in the last decade. Starting from closed cycles applied to nuclear power plants [1], the topic has been revived and further applications has been investigated and studied [2], such as integration with waste heat recovery (WHR) [3], concentrated solar power (CSP) [4], and use for energy storage [5]. It is a promising technology for which it is foreseen a high efficiency and especially high flexibility in the production and rapid adaptation to part-load needs, characteristics required in the modern energy market.

Previous studies investigated the behaviour of sCO2 cycles in part-load, as also reported in [2]. Inventory control is often shown to be efficient, despite slow and with possible stability implications [6]. Control of main mass flow trough compressor speed in a double shaft configuration is efficient and suggested in [7]. A part-load study for WHR can be found in [3], while an application to CSP of a part-load study is [8].

The present analysis follows previous works made within the SOLARSCO2OL EU project on the part-load analysis [9] and control strategy [10] of the demo cycle to be installed. In the present paper, after a presentation of the demo-cycle and the project aims, the dynamic

* Corresponding author: simone.maccarini@edu.unige.it

model developed is briefly presented, along with method to speed up the simulation. Preliminary controllers are implemented and analysed, followed by the analysis of a response of the main parameters of the plant to a ramp change in the load.

2 The Demo-Cycle and the SOLARSCO2OL Project

The SOLARSCO2OL [11] Horizon2020 European project aims at the installation and demonstration of a first-of-a-kind MW-scale sCO2 plant coupled with CSP in Europe. The sCO2 demo plant will be installed at the premises of the University of Evora and coupled with a pre-existing CSP plant using molten salts (MS) as heat transfer fluid.

The MS are heated up by the solar concentrator and then stored in a hot tank. Then, their temperature is further increased by an electric heater before entering two MS-sCO2 heat exchangers to transfer heat to the actual sCO2 plant.

The demo cycle is a simple recuperated supercritical Brayton cycle evolving CO_2. The compressor inlet conditions are fixed at 83 bar and 33°C, close to the critical point of CO_2 to reduce the compression work. The turbine inlet temperature is equal to 565°C and the maximum pressure is 188 bar. The recuperator effectiveness is set at 80%. This solution has a cycle efficiency of 21.3%. However, the study by Guedez et al. [11] demonstrated that an upscaled version of this concept could reach an efficiency higher than 31%, and adding recompression to the plant could lead to almost 50%.

3 Modelling approach

A dynamic model, described in previous works [9][10], was developed to study the off-design behaviour of the sCO2 plant using TRANSEO [12], a simulation tool developed by TPG and based on the MATLAB-Simulink environment. The model simulates compressor, turbine, sCO2-sCO2 recuperator, two MS-sCO2 heat exchangers (i.e., the heater), compressor anti-surge valve (ASV), cooler bypass valve (BCV), turbine bypass valve (BTV) and throttling valve (TTV). At this stage, the cooler is modelled as ideal by imposing 33°C at the compressor inlet.

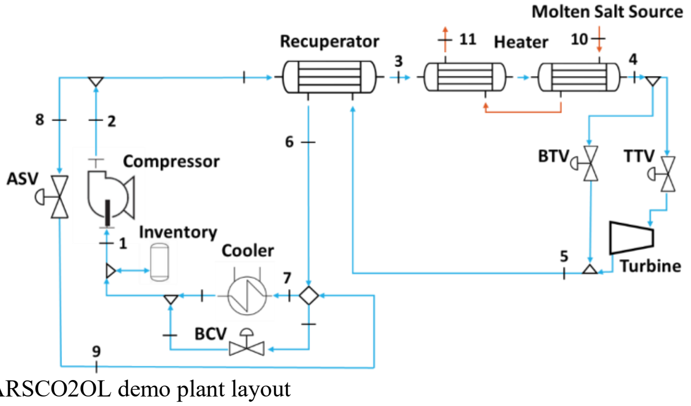

Figure 1 - SOLARSCO2OL demo plant layout

In the previous versions of this model, miniREFPROP [13] was integrated with MATLAB-Simulink and used to compute accurately the properties of CO_2 in each component. However, this approach was computationally intensive given the number of required iterations. To improve the speed of the model, miniREFPROP was used offline to create tables which map a grid of pressure p and temperature T pointing to various properties of CO_2. The tables were then implemented within some of the model components. Since the tables have a lower accuracy close to the critical point, they were only used in the models for the turbine, recuperator, and heaters, which are not expected to work in its proximity. Each one of these components computes the thermophysical properties at the desired p and T by interpolation, by fitting a plane through the four nearest p-T points on the mesh. As more precision was necessary close to the critical T and p, these tables used uneven spacing in p and T in order to maximize the density of the mesh near the critical point while minimally impacting the table size. The table spacing was determined by increasing the spacing until the error at the midpoint between each step exceeded 0.2% of its actual value for any of the properties. This error tolerance was still lenient in areas where the properties had very large variations, such as near the critical point. Therefore, outside of the table bounds, as well as very close to the critical point ($p<9$ MPa and $T<330.153$ K), miniREFPROP was called directly. Table 1 shows the reduction of computation time that is achieved using the tables, in terms of computation time ratio R_{CT}, alongside the error ε in each operating condition. R_{CT} is defined as the ratio between computation time when using the tables and the one obtained when using miniREFPROP.

Analysing Table 1, the recuperator shows the highest improvements in terms of R_{CT}, being the component with the highest number of calls to compute properties. The errors are always lower in the "Out" case, which means that many properties can be outside of the table bounds, and thus computed through miniREFPROP; anyway, the R_{CT} is below 1 since some properties can still be computed through the corresponding table. The "Nom" and "Near" cases show similar results, meaning that the dimension of the tables has a small impact on the computation time, and that the speed improvement comes from avoiding on-line miniREFPROP calls.

Table 1 - Error and R_{CT} by Component ("Nom" = Nominal conditions, "Out" = outside the table's range, "Near" = near the critical region, but within the table's bounds).

	Heater			**Recuperator**			**Turbine**		
	Nom	**Near**	**Out**	**Nom**	**Near**	**Out**	**Nom**	**Near**	**Out**
ε $T_{cold,out}$ [K]	-6.6e-3	-8.1e-4	3.4e-13	0.11	0.030	0.016	n.a.	n.a.	n.a.
ε_{max} $T_{cold,out}$ [K]	1.4e-2	4.8e-3	-3.7e-6	0.12	0.044	0.016	n.a.	n.a.	n.a.
ε $T_{hot,out}$ [K]	n.a.	n.a.	n.a.	0.048	0.010	0.016	-0.031	-0.052	0.00
ε_{max} $T_{hot,out}$ [K]	n.a.	n.a.	n.a.	0.048	0.021	0.016	-0.031	-0.036	0.00
ε $\dot{m}_{hot,out}$ [K]	n.a.	n.a.	n.a.	n.a.	n.a.	n.a.	-3.8e-3	-1.2e-3	0.00
ε_{max} $\dot{m}_{hot,out}$ [K]	n.a.	n.a.	n.a.	n.a.	n.a.	n.a.	-4.9e-3	-2.0e-3	0.00
R_{CT} [-]	0.36	0.37	0.83	0.029	0.030	0.44	0.442	0.414	0.90

4 Control development

During the operation of the plant, it is necessary to maintain a safety margin from the CO_2 critical conditions in the compressor. To do this, inlet pressure and temperature must be always kept as close as possible to the design point, even during transients. Moreover, compressor surge must be prevented. Even if the compressor model does not simulate the effect of surge, it computes the surge margin K_p, defined as the ratio between the current mass flow and the mass flow on the surge line at the current pressure ratio. It is assumed that values of K_p over 1.1 ensure safe operation of the compressor.

Given all these constraints, it is necessary to design a control philosophy able to regulate the plant and guarantee an efficient and safe operation. Based on previous off-design analyses, a control strategy was proposed by Gini et al. [10], which is resumed in Table 2.

Table 2 - Control philosophy.

Controlled variable	**Manipulated variable**
Plant net power (P_{net})	Compressor speed
Turbine inlet temperature ($T_{T,in}$)	MS mass flow rate
Compressor inlet pressure ($p_{C,in}$)	Total CO_2 mass in the loop
Compressor inlet temperature ($T_{C,in}$)	BCV opening

In this study, the controllers of P_{net}, $T_{T,in}$ and $p_{C,in}$ are designed, implemented and tested on the dynamic model. Since the cooler is modelled as an ideal component, the controller of $T_{C,}$in was not included.

In an off-design analysis in a previous work [10] the authors found that a control with a constant turbine inlet temperature leads to higher cycle efficiency; moreover, avoiding great temperature variations, a faster response is expected. For this reason, a simple feed-forward controller determines the MS mass flow necessary to reach the required $T_{T,in}$, kept to the design value, as a function of the CO_2 mass flow entering the heat exchangers. Figure 2 shows the data implemented into the feed-forward controller, in terms of percentage of the full load (FL) values. Another feed-forward controller is used to change the compressor rotational speed based on the net power demand. Later on these controllers can be integrated with a feedback loop to increase the precision.

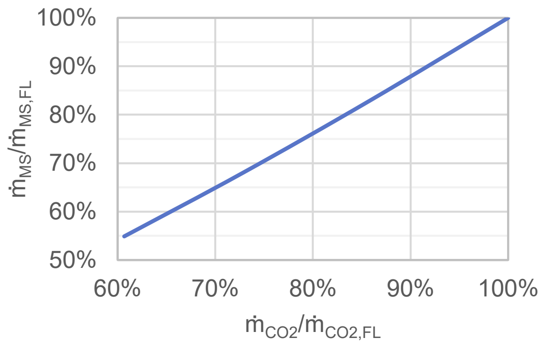

Figure 2 - $T_{T,in}$ feed-forward controller.

The pressure control is guaranteed by a simple feedback on-off controller, which changes the internal mass of the loop if the difference between actual pressure and its setpoint (83 bar) exceeds a certain limit (± 0.05 bar). If the pressure is too low, more CO_2 is introduced from the inventory, and if it is too high, some CO_2 is expelled through a venting valve. According to the plant requirements, the control can be considered effective if the pressure is always kept within ± 0.75 bar from the setpoint value. Two different solutions have been considered for this analysis: Case I, where the introduced/vented mass flow is equal to 0.1 kg/s, and Case II, where it is 0.2 kg/s.

5 Results

First of all, the model was used to simulate the full load (FL) condition. In this case, the $\dot{m}_{CO2}$ circulating in the plant is equal to 20.65 kg/s, and the $\dot{m}_{MS}$ to be provided to the heater is 19.35 kg/s. The simulation showed a generated net power P_{net} of 1456 kW with an efficiency η of 21.64%. Then the model was used to define the off-design performance of the plant, changing the compressor speed between 100% and 60% of its FL value.

Figure 3 shows the values of η, normalised over FL conditions, with respect to the variation of P_{net}. Finally, the model was used to simulate the transient operation of the plant and to verify the proper operation of the control logics. To do this, tests were carried out in different conditions, varying the net power of the plant from 100% to 50% of the FL value. The power variation follows a ramp performed over 15 minutes. Some of these tests were designed also to analyse the behaviour of the plant without some of the controllers. Table 3 shows the conditions adopted in each test. The cases of the $p_{C,in}$ control refer to the two possible solutions presented in Section 4.

During each test, the ramp variation of P_{net} setpoint translates into a variation of the compressor speed. This allows to change the mass flow rate of CO_2 in the whole cycle, which is what actually drives the net power variation, and, as a consequence, the variations of pressure ratio in the closed cycle and of temperature at the turbine inlet.

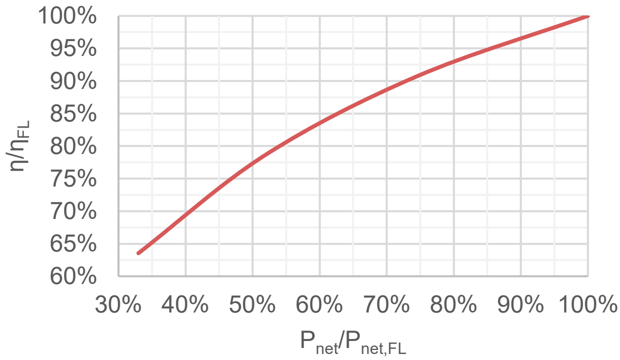

Figure 3 - Efficiency variation at part load

Table 3 – Conditions of the different transient tests.

Test case	Load Variation	Ramp duration	$p_{C,in}$ control	$T_{T,in}$ control
test a	100% → 50%	900 s	Case I	Yes
test b	100% → 50%	900 s	Case II	Yes
test c	100% → 50%	900 s	No	Yes
test d	100% → 50%	900 s	Case II	No

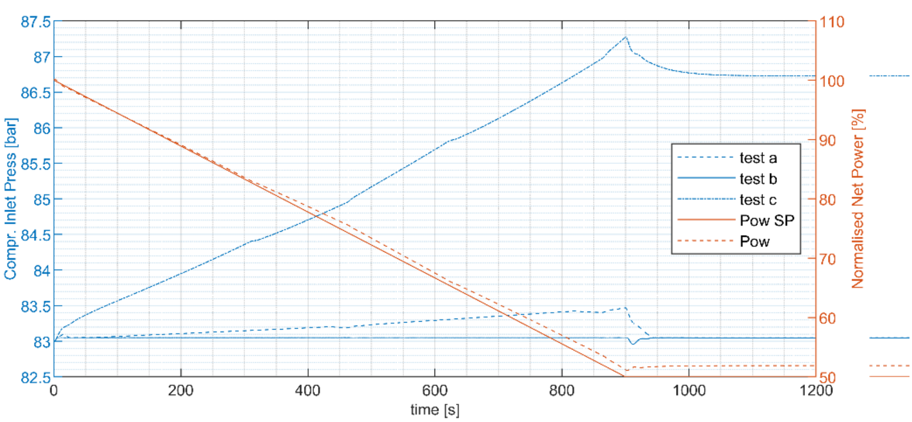

Figure 4 - Compressor Inlet Pressure with and without control implementation

Figure 4 shows the $p_{C,in}$ during the tests. Test 'c' shows the uncontrolled behaviour of the pressure, with a variation of 4 bar in response to a variation of 50% of the load. Tests 'a' and 'b' show the effectiveness of the implemented pressure control. In particular, test 'a' shows that with a CO_2 mass venting of 0.01 kg/s (Case I) the pressure value deviates from the setpoint value during the ramp, but always within the limit of ±0.75 bar. This deviation is quickly reduced to almost zero at the end of the ramp. On the other hand, test 'b' shows that a mass variation of 0.02 kg/s (Case II) leads to a stable operation of the compressor with a $p_{C,in}$ equal to 83 bar. However, this is achieved through a sudden and sometimes continuous shifts between introduction and venting of CO_2.

Figure 5 shows the surge margin behaviour during the same tests. The curve of test 'b' makes evident the alternating behaviour of the $p_{C,in}$ controller. It is important to recall that values over 1.1 represent a safe operative condition. Thus, since values of K_p lower than 1.1 were reached during all tests, further simulations will be necessary to include the effect of the anti-surge valve.

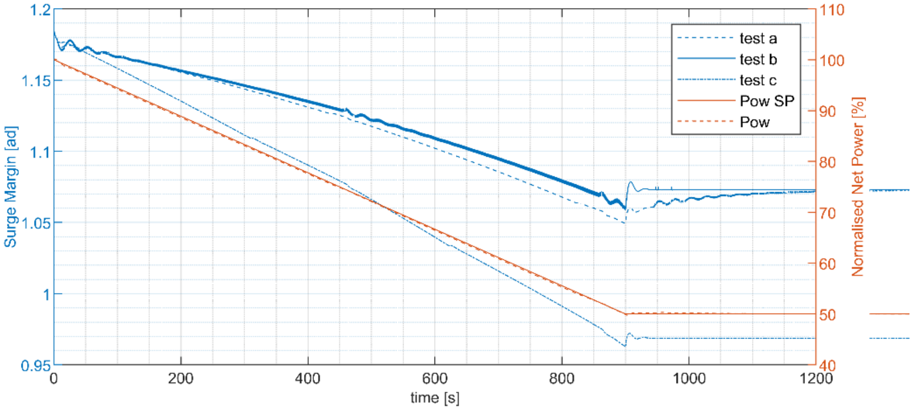

Figure 5 - Surge Margin with and without control implementation

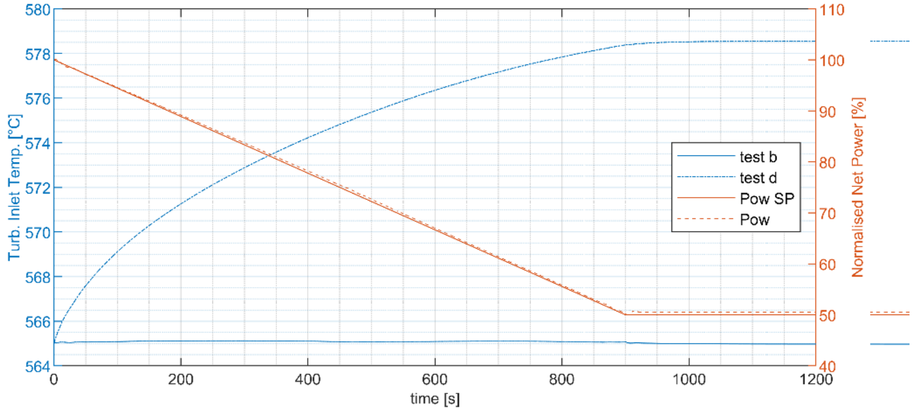

Figure 6 - Turbine Inlet Temperature with and without control implementation

Figure 6 shows the effectiveness of the control on $T_{T,in}$ control, obtained through the correlation between CO_2 and molten salts mass flow rates at the inlets of the heaters. comparing the results of test 'b' with the ones of test 'd', which shows the behaviour of the temperature without a controller. In this case the $T_{T,in}$ tends to the temperature of the molten salts, fixed at 580°C. It is important to clarify that, if a reliable measurement of the CO_2 mass flow at the heater inlet were not available in the real system, a different controller should be implemented, like a PID following the $T_{T,in}$ setpoint.

6 Conclusions

The paper presents the implementation of the controls for the compressor inlet pressure and the turbine inlet temperature of a simple recuperated sCO2 cycle.

The model is described, and tables to compute fluid properties are presented. These help to reduce the computation time, and rely on the off-line use of miniREFPROP.

The control on the compressor inlet pressure is an on-off variation of a mass flow rate from the inventory or to venting, and it allows to control the pressure through a variation of the total mass of the plant. It effectively allows a stable operation of the compressor until about 60% of load. After that, the surge margin breaks the safe region and a different control should be foreseen, for instance an intervention of the anti surge valve. Moreover, to avoid sudden variation of the control variable, a PID will also be analysed in a further study.

The control on the turbine inlet temperature is a feed-forward to control the molten salts mass flow rate given a variation of the mass flow rate of CO_2 entering the turbine. It effectively controls the temperature in all the conditions in which it is applied.

Acknowledgments

This paper has been developed in the framework of the SOLARSCO2OL project. The SOLARSCO2OL project has received funding from the European Union’s Horizon 2020 research and innovation program under grant agreement No 952953.

References

[1] Dostal, V., “A Supercritical Carbon Dioxide Cycle for next Generation Nuclear Reactors,” Advanced Nuclear Power Technology Program, MIT-ANP-TR-100, 2004.

[2] White, M. T., Bianchi, G., Chai, L., Tassou, S. A., and Sayma, A. I., 2021, “Review of Supercritical CO2 Technologies and Systems for Power Generation,” Applied Thermal Engineering, 185, p. 116447.

[3] Alfani, D., Binotti, M., Macchi, E., Silva, P., and Astolfi, M., 2021, “SCO2 Power Plants for Waste Heat Recovery: Design Optimization and Part-Load Operation Strategies,” Applied Thermal Engineering, 195, p. 117013.

[4] Crespi, F., Sánchez, D., Martínez, G. S., Sánchez-Lencero, T., and Jiménez-Espadafor, F., 2020, “Potential of Supercritical Carbon Dioxide Power Cycles to Reduce the Levelised Cost of Electricity of Contemporary Concentrated Solar Power Plants,” Applied Sciences (Switzerland), 10(15).

[5] S. Maccarini, S. Barberis, S.S. Mehdi Shamsi, L. Gini, A. Traverso, 2023. “Performance Analysis of PTES Layouts Evolving SCO2 for Industrial WHR Integrations”, The 5th European sCO2 Conference for Energy Systems, Prague, Czech Republic.

[6] “Dynamic Response of the Supercritical $C0_2$ Brayton Recompression Cycle to Various System Transients” [Online]. Available: https://dspace.mit.edu/handle/1721.1/53527 [Accessed: 21-April-2023].

[7] Luu, M. T., Milani, D., McNaughton, R., and Abbas, A., 2018, "Advanced Control Strategies for Dynamic Operation of a Solar-Assisted Recompression Supercritical CO2 Brayton Power Cycle," Applied Thermal Engineering, 136, pp. 682–700.

[8] Neises, T., 2020, "Steady-State Off-Design Modeling of the Supercritical Carbon Dioxide Recompression Cycle for Concentrating Solar Power Applications with Two-Tank Sensible-Heat Storage," Solar Energy, 212, pp. 19–33.

[9] Gini, L, Maccarini, S, Traverso, A, Pesatori, E, Milani, A, Bisio, V, Valente, R, Barberis, S, & Guedez, R. "Part-Load Behaviour and Control Philosophy of a Recuperated Supercritical CO2 Cycle." Proceedings of the ASME Turbo Expo 2022: Turbomachinery Technical Conference and Exposition. Volume 9: Supercritical CO2. Rotterdam, Netherlands. June 13–17, 2022. V009T28A019. ASME. https://doi.org/10.1115/GT2022-83021

[10] Gini L., Maccarini S., Traverso A., Barberis S., Guedez R., Pesatori E., Bisio V., "A prototype recuperated supercritical co2 cycle: Part-load and dynamic assessment", Applied Thermal Engineering, Volume 225, 2023, 120152, ISSN 1359-4311, https://doi.org/10.1016/j.applthermaleng.2023.120152.

[11] Guédez, R, Barberis, S, Maccarini, S, López-Román, A, Milani, A, Pesatori, E, Oyarzábal, U, & Sánchez, A. "Design of a 2 MW Molten Salt Driven Supercritical CO2 Cycle and Turbomachinery for the SOLARSCO2OL Demonstration Project." Proceedings of the ASME Turbo Expo 2022: Turbomachinery Technical Conference and Exposition. Volume 9: Supercritical CO2. Rotterdam, Netherlands. June 13–17, 2022. V009T28A008. ASME. https://doi.org/10.1115/GT2022-82013

[12] Traverso, A., 2005, "TRANSEO Code for the Dynamic Performance Simulation of Micro Gas Turbine Cycles," Proceedings of the ASME Turbo Expo, 5, pp. 45–54.

[13] miniREFPROP https://trc.nist.gov/refprop/MINIREF/MINIREF.HTM [Accessed: 21-April-2023].